Simulation of Glassy State Relaxations in Polymers: A Static Analysis of Methyl Group and Methoxy Group Rotation in Poly(vinyl methyl ether)

Jean-Claude Berthet,[†] Cherdsak Saelee,[‡] Taining Liang,[§] Timothy M. Nicholson,[⊥] and Geoffrey R. Davies*[,#]

Science Institute VR2, University of Iceland IS-107, Reykjavik, Iceland; Department of Physics, Chiang Mai University, Chiang Mai, 50200 Thailand; Department of Chemistry, Centre for Scientific Computing, University of Warwick, Coventry, CV4 7AL; Division of Chemical Engineering, University of Queensland, Brisbane 4072, Australia; and Polymer IRC, School of Physics, University of Leeds, Leeds LS2 9JT, UK

Received June 27, 2006; Revised Manuscript Received August 23, 2006

ABSTRACT: We show that the simple quasi-static technique, also called the adiabatic mapping technique, can be used to determine the energetics of rotation of methyl and methoxy groups in amorphous poly(vinyl methyl ether) even though the latter process is too slow to be amenable to direct molecular dynamics simulation. For the methyl group rotation, we find that the mean and standard deviation of the simulated rotational barrier heights agree well with experimental data from quasi-elastic neutron scattering. In the case of the methoxy groups we find that just 4% of the groups contribute more than 90% of the observed dielectric relaxation strength. The groups which make the most contribution are those which, by virtue of their particular conformation and local environment, have two alternative positions of similar energy.

1. Introduction

Prior to the advent of direct molecular dynamics simulation, experimentalists proposed a variety of molecular mechanisms for the different relaxations seen in polymers, often disagreeing widely from one to another. Force fields, molecular dynamics (MD) techniques, and computing capability have now developed, however, to the point where sufficiently rapid relaxations can be directly simulated, albeit at high temperatures. See, for example, the recent simulation of dielectric relaxation in polybutadiene.[1]

In this publication, however, we are interested in relaxations occurring deep in the glassy state such as the β relaxation in poly(vinyl methyl ether) (PVME) which has a dielectric relaxation time[2] of 4 μs at 150 K. This is currently too slow to be directly simulated by molecular dynamics techniques with sufficient atoms to simulate a significant volume of amorphous PVME. It is possible, of course, to simulate the process at high temperatures, in the region where the secondary relaxations merge with the glass transition,[1,2] but such temperatures are not representative of the glassy state. We show in this paper, however, that the quasi-static (QS) technique[3,4] can be used to determine energy barriers to both methyl and methoxy side group rotation at 0 K and that this method yields data in good agreement with experiments at low temperatures.

We have previously shown that the method may successfully be applied to methyl group rotation in PMMA[5] where comparison of MD simulations and experiment gave encouraging results. Experimental data and hence simulation data were, however, analyzed with the Kohlrausch−Williams−Watts (KWW) function.[6] This function gives a nonintuitive estimation of the spread of activation energies through the departure of its β parameter from unity. Comparison of experimental and simulated β parameters is therefore somewhat unsatisfactory since the significance of a slight disagreement is difficult to appreciate in physical terms, and the value of the β parameter is thus a rather insensitive test of the validity of the simulation.

Experimental data for both methyl group rotation[7] by quasi-elastic neutron scattering (QENS) and methoxy group rotation[2] by dielectric spectroscopy in PVME have, however, been analyzed in terms of the rotation rate distribution model (RRDM) which effectively assumes that the distribution of energy barriers is Gaussian and utilizes the width of this distribution as a fitting parameter. We have therefore applied the QS technique to these processes and analyzed our simulation in terms of the RRDM to allow a more physically meaningful comparison of the QS simulation technique with experiment. To help appreciate the temperature dependence of the distribution of energy barriers, we have also used dihedral angle distribution analysis (DADA) of short MD runs.

Our methyl group analysis has been limited to the determination of energy barriers to rotation, assuming that the strength of the contribution is the same for each methyl group. This is reasonable since the energy of a group before and after rotation is the same since the group effectively fits back in the same "hole" in its environment after a 120° rotation. For the methoxy group, however, the energy before and after rotation can be widely different, resulting in a vast range of effective polarizabilities for each group. We have therefore calculated the total dielectric relaxation strength from our simulations and shown good agreement with experiment. We will present a more complete treatment of the methoxy group data in a separate publication[8] which generates a complete reconstruction of the dielectric loss curve as a function of frequency for the β relaxation which is in excellent agreement with results from dielectric experiments.[9]

* To whom all correspondence should be addressed. E-mail: g.r.davies@leeds.ac.uk.
[†] University of Iceland.
[‡] Chiang Mai University.
[§] University of Warwick.
[⊥] University of Queensland.
[#] University of Leeds.

10.1021/ma061442j CCC: $33.50
Published on Web 10/12/2006

2. Simulation Cell Construction

The simulation cells for the methyl group study were those used in a previous publication[10] reporting the results of molecular dynamics simulations of methyl group rotation in PVME. These cells were built using the InsightII software from MSI with the PCFF2 force field. Each cell contained an atactic polymer chain of 180 repeat units with a chiral inversion probability of 0.64, comparable with experimental material. Cells were initially built at 500 K and then cooled to 200 K while running NPT MD. Cell 1 was cooled in 25 K steps, allowing 100 ps at each step, while the other four cells were cooled in 100 K steps with a run of 1 ns at each step. Group-based cutoffs of 8.5 Å were used for both Coulomb and van der Waals interactions with a spline width of 1 Å and a buffer width of 0.5 Å. A tail correction was applied to correct for the effect of the cutoff on the simulation pressure. The mean density of the five cells was 1.058 g/cm^3 with a standard deviation of 0.004 g/cm^3. This is somewhat less than the experimental value[11] of 1.085 g/cm^3 at 200 K, as might be expected from the high simulation cooling rate.

The simulation cells used for analysis of the methoxy group rotation were generated some time later with the Materials Studio software from Accelrys using the COMPASS force field,[12] this software and force field being a more modern development of that used for the methyl group study. A total of six cells were generated, each containing a 250 repeat unit atactic chain with the above chiral inversion probability. The cells were built using the amorphous cell constructor at 500 K and a low density of 0.8 g cm^{-3} before running NPT MD for 100 ps at 500 K to allow the cells to reach their equilibrium density around 0.9 g cm^{-3}. The cells were then cooled from 500 to 150 K in steps of 25 K by running 100 ps of NPT MD at each temperature. Temperature was controlled by an Andersen thermostat,[13] and pressure was controlled by the Berendsen barostat.[14] The velocity Verlet integrator was used with an integration step of 1 fs. In view of the larger size of the rotating group, somewhat larger group-based cutoffs of 9.5 Å were used.

3. The Quasi-Static Method

In the QS method, a dihedral angle is forced to a desired angle by the addition of an extra "forcing" potential to the system energy expression, and the total energy of the system in the presence of this forcing term is minimized with respect to all coordinates. Repeated evaluation of the total energy (without the contribution from the forcing potential) at different forced angles yields the minimized energy as a function of dihedral angle.

The quasi-static method is frequently used to study the energetics of bond rotations in small molecules but has seen little application in polymers. It was first used to study the rotation and oscillation of the phenyl ring in the glassy polystyrene[3] with little experimental justification, but comparison with MD and experimental studies of methyl group rotation in PMMA[5] showed that the QS method yielded comparable data and was worthy of further study.

The simplest and most commonly used functional form for the forcing potential is a simple quadratic function:

$$U_{\text{forcing}}(\varphi) = k_{\text{forcing}}(\varphi - \varphi_{\text{target}})^2 \qquad (1)$$

where k_{forcing} is a force constant, φ is the current dihedral angle, and φ_{target} is the target dihedral angle. If the force constant k_{forcing} is large enough, then after energy minimization the dihedral angle will be close to the target value.

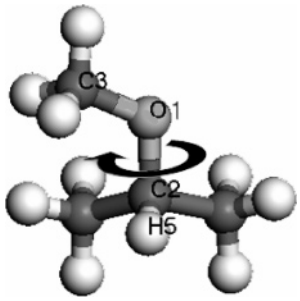

Figure 1. Methoxy rotation. The C2−O1 bond is the rotating bond.

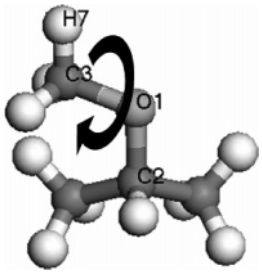

Figure 2. Methyl rotation. The O1−C3 bond is the rotating bond.

The dihedral angle chosen to rotate the methoxy group is indicated in Figure 1 by the atoms H5−C2−O1−C3. The force constant k_{forcing} was set to 1000 kcal/mol/rad.

In the case of the methyl group, torsion restraints were originally applied to the dihedral angles for each hydrogen atom separately with target dihedrals being measured from the starting position of each hydrogen atom. Forcing all atoms to rotate through the same angle at each step proved to overconstrain the system, however, and yielded somewhat high barriers. It was found to be better to apply a forcing potential to the average dihedral angle turned through, thus giving a more flexible rotor. A natural form for this average torsional restraint was a 3-fold harmonic function:

$$U_{\text{forcing}}(\varphi) = V[1 + \cos(3(\varphi - \varphi_{\text{target}}))] \qquad (2)$$

where V gives the strength of the restraint, φ is the average angle turned through by the three hydrogen atoms, and φ_{target} is target angle. The use of the lowest possible value for V sufficient to ensure reasonable approach to the target angle allows the individual hydrogen dihedral angles to vary as the group rotates.

3.1. Energy Minimization. All minimizations were performed using the commercial software package Discover from Accelrys. Minimizations commenced with the robust but slow steepest descent method and switched to the faster conjugate gradient method when the gradient was low enough.

Cells taken from the low-temperature MD runs were initially minimized to a maximum derivative less than 0.001 kcal mol^{-1} Å^{-1} prior to applying the QS technique. Experimentation showed that the subsequent QS minimizations could be ceased when the maximum derivative was less than 0.01 kcal mol^{-1} Å^{-1} with little effect on the observed energy barriers.

3.2. The Dihedral Angle Step. Initial studies mapped out the energy of a rotating methyl group as a function of dihedral angle every 2°. It was found, however, that increasing the step to 10° reduced the simulation time by a factor of 2 with little loss of accuracy provided that energy and position of the top of the barrier (transition angle) were calculated by fitting the three points nearest the top of the barrier, as shown in Figure 3. The speed-up was less than the naively calculated factor of

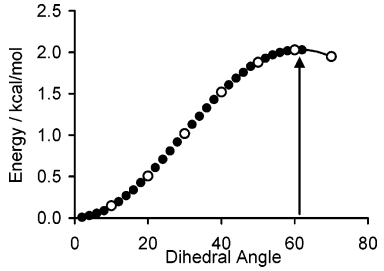

Figure 3. QS rotation of a methyl group. Black dots are from 2° steps. White circles are from 10° steps. The line is a quadratic fit to the three points near the top of the barrier.

Table 1. Mean Energy Barrier and Standard Deviation before Cleaning, after Cleaning, and for a Gaussian Fit after Cleaning (All Data in kcal/mol)

	density,	raw results		after cleaning		Gaussian	
cell	g/cm^3	mean	SD	mean	SD	mean	SD
1	1.064	2.191	0.595	2.216	0.572	2.135	0.457
2	1.058	2.112	0.517	2.128	0.484	2.132	0.400
3	1.051	2.190	0.550	2.215	0.524	2.127	0.381
4	1.057	2.130	0.510	2.152	0.481	2.094	0.457
5	1.061	2.164	0.548	2.179	0.530	2.119	0.476
all	**1.0582**	**2.157**	**0.545**	**2.178**	**0.521**	**2.123**	**0.436**

5 since each minimization took longer because the departure from equilibrium was greater.

4. Methyl Group Rotation Studies

4.1. Cleaning. The QS technique was applied to all methyl groups in five cells (a total of 900 groups), rotating them until the first maximum was just passed. The results showed some particularly high or low barriers. It is sensible to ask whether such data should be included in any further analysis. To help identify "unusual" results, the transition angle was also considered. All groups which had an energy barrier or transition angle deviating by more than one and a half standard deviations from the average were treated as suspicious. For these groups, about 20% of the total, extended runs were performed to determine the energy as a function of torsion angle over a complete 360° rotation. Some showed unusual barriers but with 3-fold symmetry and a reasonable transition angle. These units were accepted whereas those showing no symmetry or a transition angle more than 3 times the standard deviation away from the average value were rejected and removed from any further calculations.

4.2. Distribution of Energy Barriers. Most of the groups that were discarded had a low energy barrier and low transition angle. Consequently, the mean energy increased slightly, and the standard deviation decreased slightly after elimination of these data, as seen in Table 1. Clearly, however, cleaning has little effect on the mean and standard deviation.

Also given in Table 1 are the densities of the cells. It can be seen that they cover a relatively narrow range, and no correlation of energy barrier or its standard deviation with density is apparent.

Figure 4 shows a histogram of the distribution of energy barriers together with a Gaussian fit. Clearly the distribution is slightly asymmetric, being broader on the high energy side. The deviations from a Gaussian distribution are not great, but the standard deviation resulting from the Gaussian fit clearly underestimates the actual breadth of the distribution.

The distribution of the transition angle for all accepted groups is plotted in Figure 5 and fitted by a Lorentzian distribution function. Average transition angles are ~60°, as expected.

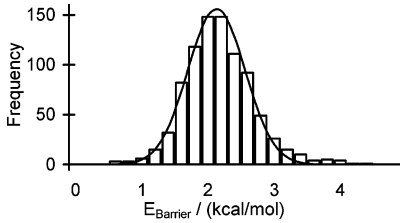

Figure 4. Distribution of energy barriers (874 groups in all). The continuous line is a Gaussian fit.

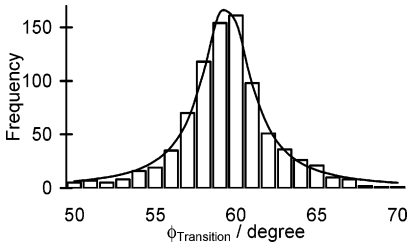

Figure 5. Distribution of transition angles after cleaning. The continuous line is a Lorentzian fit.

The experimental data[7] arising from an RRDM fit to QENS data from 180 to 300 K yield a mean barrier of 2.01 kcal/mol with standard deviation of 0.41 kcal/mol at 200 K. It is not surprising that the simulation yields a close mean barrier of 2.1−2.2 kcal/mol, depending upon the degree of cleaning of the data, since this figure is dominated by the force-field parametrization for the dihedral angle stiffness, with little contribution from the environment terms. The width of the distribution is, however, determined by the amorphous environment, and here we obtain an excellent prediction of 0.44−0.54 kcal/mol.

It is reasonable to ask to what extent the difference is due to the effects of temperature since the QS method is effectively a 0 K method while experiments were conducted around 200 K. To explore this possibility, we used dihedral angle distribution analysis of MD runs at different temperatures—effectively generating a potential of mean force for each individual methyl group at each temperature.

4.3. Dihedral Angle Distribution Analysis (DADA). In this section we determine the energy, $E(\phi)$, of a methyl group as a function of its angle of rotation by observation of the dihedral angle distribution function during MD runs. To reduce the required running time, we assume that the energy profile is 3-fold symmetric and hence do not need to wait for a methyl group to sample all three minima but simply analyze the minimum that each group is currently in.

According to Boltzmann statistics, $P(\phi)$, the probability of finding a group at a dihedral angle ϕ is related to $E(\phi)$ by

$$P(\phi) = P_0 \exp\left(\frac{-E(\phi)}{k_B T}\right) \tag{3}$$

Although the form of the function $E(\phi)$ is unknown, it was found that it was well represented by

$$E(\phi) = \frac{E_{\text{barrier}}}{2}(1 - \cos[3(\phi + \delta)]) \tag{4}$$

The probability function $P(\phi)$ was determined by analyzing the MD runs used to cool the cells, the last 60 ps of the 100 ps of data taken at each temperature being used. Since the number of observations at a given angle varied strongly with angle, the fitting parameters P_0, E_{barrier}, and δ were determined by a

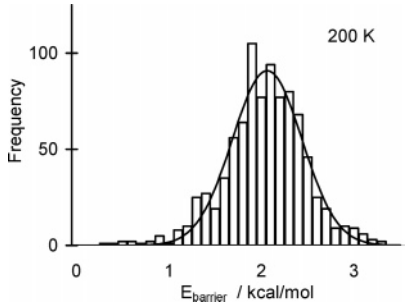

Figure 6. Energy barrier distribution obtained by DADA analysis at 200 K together with Gaussian fit.

Table 2. Mean Energy Barrier, E_b (in kcal/mol), and Offset Angle, δ (in deg), with Their Respective Standard Deviations, σ_i, at Different Temperatures

	data		Gaussian fit	
T/K	E_b	σ_E	E_b	σ_E
500	1.784	0.139	1.799	0.143
400	1.859	0.220	1.891	0.206
300	1.948	0.344	1.991	0.314
200	2.088	0.434	2.112	0.376

	data		Gaussian fit	
T/K	δ	σ_δ	δ	σ_δ
500	−0.036	0.907	−0.050	0.883
400	0.009	1.820	0.006	1.450
300	0.163	3.036	0.044	2.538
200	0.348	4.339	0.226	3.541

weighted least-squares fitting of the observed probability to that predicted from use of the above equations.

Since we analyzed NPT simulations, we determined a Gibbs free energy rather than an internal energy. The resulting energy barriers were binned in 0.1 kcal/mol bins in order to produce a barrier distribution at temperatures of 500, 400, 300, and 200 K, and an example is presented in Figure 6. The distributions were well fitted by a Gaussian, and the full fitting results are summarized in Table 2.

The energy barrier distributions show an increase in mean value with reducing the temperature, together with a strong broadening of the distribution. The mean offset angle is essentially zero, being much less than its standard deviation, but the standard deviation broadens with decreasing temperature. All of these effects presumably arise due to the increasing importance of the steric hindrance imposed by each group's local environment as temperature is reduced.

4.4. Comparison of QS with DADA and Experiment. When comparing the two approaches, it must be remembered that the QS approach is essentially a determination of the energy barriers at absolute zero. Since the DADA-derived quantities are temperature-dependent, the extrapolated values should be compared. A compact comparison of the energy barriers and widths of the distributions is shown in Figure 7, which plots the width of the distribution as a function of the energy barrier. Clearly, the width of the distribution and the mean barrier height decrease as the temperature increases. Since we have generated a Gibbs free energy, the reduction in mean barrier height is indicative of a positive entropy contribution, ΔS, to the free energy barrier of 1.0 ± 0.1 cal/mol and an enthalpy change, ΔH, of 2.27 ± 0.04 kcal/mol. Such a low value for ΔS is consistent with a small side-group noncooperative motion.[15] The ΔH is close to the calculated QS result of 2.18 kcal/mol, and thus the results of both approaches are consistent with each other and with the experimental data shown as the open triangle in Figure 7. The simulated distribution of energy barriers is shown in Figure 8. The temperature dependence of the width of the distribution determined by DADA yields an enthalpy change of 0.64 ± 0.02 kcal/mol and an entropy change of 1.0 ± 0.1 cal/mol, consistent with that derived from the mean barrier. The temperature dependence of the free energy seen in the simulations was not reported experimentally due to the method of analysis of the data which generated an activation enthalpy.

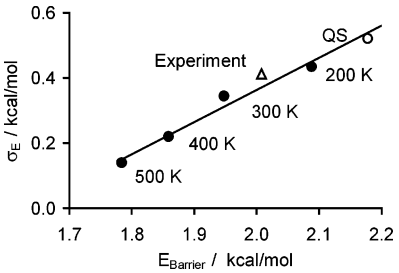

Figure 7. Energy barrier standard devation, σ_E, vs mean energy barrier. Solid points from DADA, open circle from QS, and open triangle from experiment.

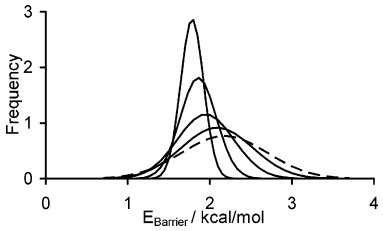

Figure 8. Energy barrier distributions from DADA (solid line). In decreasing order of peak height, the temperatures are 500, 400, 300, and 200 K. The dotted line is the distribution from the QS rotation (effectively 0 K).

Table 3. Mean Energy Barrier and Standard Deviation from Different Methods[a]

	E/kcal/mol	σ_E/kcal/mol
QS	2.18	0.52
DADA 0K	2.27	0.64
DADA 200K	2.09	0.43
TR	2.01	0.37
RRDM	2.27	0.44
QENS	2.01	0.41

[a] DADA 200K, TR, and RRDM data are at 200 K. QS and DAD 0K are at 0 K. TR and RRDM are values from Saelee.[10] The QENS experimental[7] data are 180−300 K with the standard deviation at 200 K.

4.5. Conclusions for Methyl Group Rotation Studies. As summarized in Table 3, in this paper and our previous work[10] we have now investigated four alternative ways of obtaining the distribution of energy barriers to methyl group rotation by simulation, all in reasonable agreement with each other and with experiment.

It is not surprising that the QS technique works for such a small, symmetric object as a methyl group which requires no rearrangement of its environment to accommodate the group after rotation. This work was primarily undertaken as a validation of the QS technique in a situation amenable to a variety of other simulation techniques. With these encouraging results obtained, however, we can proceed to see whether the QS technique is able to deal with rotation of the larger, slower, and asymmetric methoxy group where MD studies are essentially impossible, but experimental dielectric relaxation data provide an excellent target for simulation.

CDV

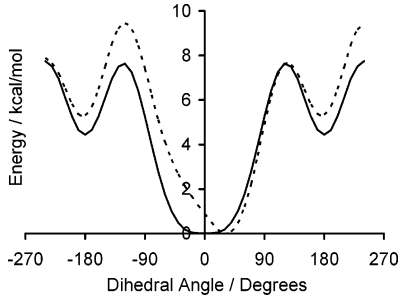

Figure 9. Methoxy group rotation energy profiles. The solid line is the average profile, and the dotted line is the average when data are treated to make the main minimum occur at a positive angle as described in the text.

5. Methoxy Group Rotation Studies

Two different series of QS simulations were performed on the methoxy groups. In the first series most of the methoxy groups of the six cells were rotated. The second series was a computationally more expensive simulation and was applied only to a selected set of groups chosen on the basis of results provided by the first simulation. The dipole moment of both the cell and the rotating group was recorded during the QS rotations to allow dielectric data to be calculated from the energy profiles. Details common to both QS simulations have already been presented above. We present below only those details which differ.

5.1. The First Series "Full" QS Simulation. In this series, the QS technique was applied to all methoxy groups in six different simulation cells apart from those at the ends of the chain. The molecular weight (M_W) of PVME has been estimated[7,16] as ranging from 63 000 to 113 000. This is equivalent to chains with 1000−2000 repeat units rather than the 250 repeat units per chain used here. The groups in the two end units were not therefore included in the simulation since they are normally a factor of 4−8 less common in real PVME.

Cells were built generally as described above, but the van der Waals and group-based Coulomb interaction cutoffs were both set to 9.5 Å. Denser than average frames were chosen from the 200 K MD trajectories for final minimization to yield a mean density over five of the cells of 1.093 g/cm^3 with a standard deviation of 0.008 g/cm^3. One cell with the extremely low density of 0.931 g/cm^3 was also studied.

In the subsequent QS simulations atoms further than 14 Å from the rotating group's oxygen atom were held fixed during the minimizations for computational speed. (This radius will be referred to as the "fix radius".) Starting from its initial position, each methoxy group was forced in both direction to the absolute angle value −240° and +240° measured with respect to the hydrogen atom H5 in Figure 1.

The results from these simulations showed wide variations in the individual energy profiles, but the average energy profile, displayed in Figure 9, is smooth and symmetrical with one broad minimum around 0° and another at ±180°. (The 0° minimum is, in fact, two minima separated by an extremely low barrier at 0° ∼ 10^{-3} kcal/mol, which is negligible for all intents and purposes.) The ±180° minimum is sharper and 4.4 kcal/mol higher. Two symmetric barriers, 7.7 kcal/mol above the minimum at 0°, separate the two minima.

Individual profiles are highly asymmetric, however, and differ greatly from the average profile. Because the minima on the average profile are located around 0° and −180° or +180°, we shall refer to these minima as 0°, +180°, or −180° minima for the individual profiles, even though their position might not be where it is indicated by this nomenclature. In fact, the 0° minimum is widely distributed within the interval −50° to +50°.

Initial inspection of individual profiles suggested a correlation of the barrier height with the position of the 0° minimum in that the barrier at −120° tended to be higher when the 0° minimum was on the positive side of zero and vice versa. This was investigated by rotating about the vertical axis those profiles which had their 0° minimum at a negative angle (such that the minimum was then at a positive angle) before computing the average profile. The result, displayed as the dotted line in Figure 9, shows a strong asymmetry in that the barrier next to the 0° minimum tends to be lower, at 7.6 kcal/mol, while the other barrier is 9.4 kcal/mol. The position of the 0° minimum is now 30°. We assume that the higher angle barrier is related to the greater angle through which the group has to turn, thus straining the environment more. Somewhat surprisingly, given this large asymmetry, the energy of the ±180° sites is essentially the same at 5.3 kcal/mol, no matter by which of the barriers they are accessed.

In view of this strong asymmetry, the naive average profile shown in Figure 9 is not representative of the profile for an individual group. Profiles are more like the asymmetric profile, if suitably inverted when required, but there is still a massive variability in the individual profiles. This variability means that we cannot assume that each group makes the same contribution to the dielectric relaxation strength but must separately calculate the contribution of each group.

5.2. Dielectric Relaxation Strength Analysis. The strength of a dielectric relaxation is measured by the step in relative permittivity, $\Delta\epsilon_r$, or susceptibility, $\Delta\chi_r$, as the measurement frequency is increased from a low frequency (where the dipoles have ample time to respond to the applied electric field) to a high frequency (where they have no time to respond before the field is reversed). The polarizability, α_i, of a dipole of moment, $\boldsymbol{\mu}_i$ (bold indicates a vector quantity), is given by

$$\alpha_i = \frac{\langle(\delta\boldsymbol{\mu}_i)^2\rangle}{3kT} = \frac{\langle\boldsymbol{\mu}_i^2\rangle - \langle\boldsymbol{\mu}_i\rangle^2}{3kT} \tag{5}$$

where the angular brackets imply ensemble averaging. Ignoring local field effects for the moment, the relaxation strength is simply given by

$$\Delta\epsilon_r = \Delta\chi_r = \frac{1}{V\epsilon_0}\sum_i \alpha_i = \frac{1}{V\epsilon_0}\sum_i \frac{\langle\boldsymbol{\mu}_i^2\rangle - \langle\boldsymbol{\mu}_i\rangle^2}{3kT} \tag{6}$$

where V is the volume of the system, ϵ_0 is the permittivity of free space, and i runs over all groups in the system. The omission of the two end units from a chain of 250 units is corrected for by multiplying the relaxation strength calculated above by the factor 250/248. The probable random error in the relaxation strength is calculated from the standard error in the average polarizability.

Calculations of relaxation strength are usually performed in terms of simple "site models" where a dipole may reside in a small number of states or sites, frequently as few as two, with different energy and dipole moment. It the present case, it is not clear whether the minimum reached by a negative rotation should be considered as the same state as the one reached by a positive rotation since the forced rotation can provoke a rearrangement of the whole structure. The problem is similar to that of turning a screw in a nut where half a turn in either direction clearly leads to different states due to translation. We might imagine that during the rotation some atoms are in the

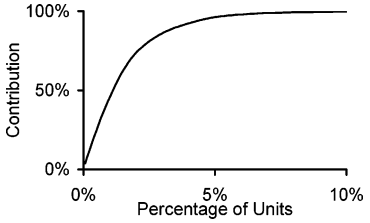

Figure 10. Cumulative contributions to the predicted relaxation strength.

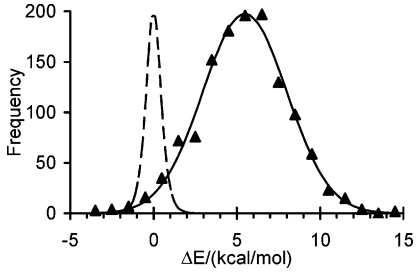

Figure 11. Energy difference distribution. Triangles from simulation. Continuous line is a Gaussian fit. The dashed line shows the term $\cosh^{-2}(\Delta E/2kT)$ (on an arbitrary scale).

way of the rotating group. The hindering atoms may be displaced during the rotation, and it is probable that a different group of atoms will be displaced by a rotation in the opposite direction leading to different microscopic states. In view of this dilemma, it was eventually decided to perform both two-site and three-site calculations though initial analysis concentrated on the two-site model.

In the two-site model, the energy and dipole moment for the sites at $-180°$ and $+180°$ were each averaged to produce a single $\pm 180°$ site. The susceptibility was then calculated using the two sites at $0°$ and $\pm 180°$.

In the particular case of the two-site model, eq 5 becomes

$$\alpha = \frac{(\boldsymbol{\mu}_{0°} - \boldsymbol{\mu}_{\pm 180°})^2}{12k_{\mathrm{B}}T\cosh^2\left(\frac{\Delta E}{2k_{\mathrm{B}}T}\right)} \tag{7}$$

where ΔE is the energy difference between the two sites. This equation clearly demonstrates the importance of ΔE in determining the polarizability of a given group. Only groups with ΔE comparable to or less than $k_{\mathrm{B}}T$ can make a significant contribution to the results.

5.3. Results for the Full QS Simulation. Because the structure used for the QS was equilibrated at 150 K, the relaxation strength was calculated at that temperature. Applying the two-site model, the calculated relaxation strength was 0.068 $\pm$ 0.01. This is comparable with the experimental value[9] of 0.12 $\pm$ 0.01 but well outside the range of statistical and experimental error. Moreover, the standard error in the simulation result was relatively large at 14% even for a simulation over six cells containing 1500 groups in all.

The large error arises because most groups contribute little or nothing to the relaxation strength due to the strong influence of the ΔE term in the susceptibility. However, a few groups make a large contribution leading to an average roughly comparable with the experimental value. It was found that 4% of the groups contributed 90% of the response with 50% coming from just 1% of the groups. The cumulative contribution is shown in Figure 10.

Why so few groups contribute is highlighted by plotting the distribution of energy difference as is done in Figure 11, where the triangles represent the distribution of energy difference between the two minima. The full line is a Gaussian fit of the distribution. The average energy difference is 5.4 kcal/mol while the standard deviation is 2.6 kcal/mol. The dotted line represents the effects of hyperbolic cosine term appearing in eq 7. In other words, it represents the relative contribution of a group as a function of the energy difference ΔE. It shows that when the energy difference ΔE differs by more than a few $k_{\mathrm{B}}T$ from 0 that group's contribution is negligible. Although the energy difference for most of the units is too high for them to have any noticeable effect on the susceptibility, a few groups in the tail of the distribution lie in the region of high contribution. It is these few groups which give PVME its observed dielectric relaxation.

This explains why previous work[17] undertaken to model the rotation of large side groups in PMMA gave unsatisfactory results in that the strength of the predicted process was apparently too small. It was proposed that the disagreement came from a lack of rearrangement in the environment on the time scale of the simulations although the simulators had attempted to minimize this problem by using the umbrella sampling method. In our view, however, the lack of agreement was caused by sampling too few groups to locate those which made significant contribution to the relaxation strength. With the benefit of hindsight, the computing time devoted to the computer-intensive umbrella sampling runs would probably have been better spent studying many more groups by the QS method.

We originally worried about the effects of the correlations between dipoles since, in a local field model, the important parameter would be the autocorrelation function for the whole cell dipole moment leading to terms in $\langle \delta\mu_i \delta\mu_j \rangle$, where μ_i is still an individual group dipole moment. Investigation of the importance of terms where $i <> j$ showed, however, that such terms could safely be neglected. In effect, the low density of highly contributing groups means that they are rarely close enough together to yield strong correlation effects.

5.4. The Limited QS Simulation. Originally, to study all groups, we used a 9.5 Å cutoff and fixed all atoms more than 14 Å away from the rotating group. In this second series of simulations, we attempted to improve our predictions by relaxing these restrictions. The cost in time required to improve the simulations was compensated for by considering only those groups which were found to contribute significantly to the relaxation strength.

The 30 most contributing groups from each cell were chosen for the limited simulation series. These groups were responsible for more than 99% of the total relaxation strength. In the new simulation, the van der Waals and Coulomb cutoff was raised to 12 Å, and no atoms were held fixed during the minimizations.

5.5. Results of the Limited QS Simulation. The results for this limited simulation were analyzed in terms of both two-site and three-site models. For the latter model, some units had to be rerun. It was assumed in the early simulation that a group always started in its $0°$ minimum. As it turned out, a few groups started in a $\pm 180°$ position. This is immaterial in a two-site model, but to be consistent with our justification of the three-site model, the three sites should be either $-360°$, $-180°$, $0°$ or $-180°$, $0°$, $+180°$, or $0°$, $+180°$, $+360°$ depending upon the initial position. Where required, some of the groups were rerun to satisfy this.

All of the results, including those from the first simulation, are summarized in Table 4. It can be seen that reducing the restrictions in the second series of simulations improves the

Table 4. Comparison of Simulated Relaxation Strength with Experimental Value[2]

method	$\Delta\epsilon$	error
full two-site	0.068	0.010
limited two-site	0.096	0.014
limited three-site	0.117	0.014
experiment	0.120	0.010

Table 5. Density of Cells and Weighted Activation Energy

cell	density, g/cm^3	weighted activation energy, kcal/mol
1	1.087	4.415
2	1.083	4.208
3	1.096	4.851
4	1.103	4.558
5	1.095	4.432
mean	1.093	4.49
SD	0.008	0.24
6	0.931	4.82

agreement with experiment, and a three-site analysis achieves almost exact agreement with experiment (almost certainly somewhat fortuitously in view of the probable errors in both!)

5.6. Activation Energy. Previously, a simple average activation energy for the methyl group rotation was calculated since it was assumed that each group contributed equally to the relaxation strength. The problem is, however, much more complex for the methoxy group. The group has two states with different energies which vary widely from group to group. Sometimes, the $\pm 180°$ minimum is lower in energy, sometimes it is higher by as much as 10−11 kcal/mol, or it may even not be present. Since the energy difference determines the contribution of the group to the relaxation strength, a simple average of the activation energy from the barrier profiles is unlikely to give the correct activation energy.

In this paper we report an average activation energy, weighted by the term $\cosh^{-2}(\Delta E/2kT)$ since the effects of differences in dipole moment change are small compared with this. The average activation was calculated from

$$\langle E_{\mathrm{act}} \rangle = \sum_i \frac{E_{\mathrm{act},i}}{\cosh^2\left(\frac{\Delta E_i}{2k_{\mathrm{B}}T}\right)} \tag{8}$$

where $E_{\mathrm{act},i}$ is the activation energy of the dipole. In the two-site model this is essentially the difference between the higher minimum and the top of the lowest barrier between the two sites. The average activation energy over the six cells obtained by this method is 4.38 kcal/mol or 18.3 kJ/mol.

This is gratifyingly comparable with the experimental values of 21.23 kJ/mol reported by Gomez et al.[2] and 21.70 kJ/mol reported by Cendoya et al.[9] However, to have an activation energy determined in a manner which is truly compatible with the experiments, a complete dynamic analysis is necessary. This work will be reported in a subsequent paper[8] which describes our approach to performing a full dielectric frequency response analysis from the rotational energy and dipole moment profiles of each group.

It might be expected that there is a correlation of the activation energy with the cell density. The cells used in the initial methyl group rotation study had a narrow range of densities, and no trend was apparent. The cells used for the latter methoxy group studies included one extremely low-density cell, and hence the weighted average activation energies were computed on a cell by cell basis to investigate the possibility of a density dependence of the activation energy.

It can be seen from the data in Table 5 that cell 6 has a lower density but a higher activation energy than the averages for cells 1−5. The departure from the average activation energy is only about one and a half standard deviations, however, and cell 3, with a higher than average density, has the highest activation energy, even higher than cell 6. It would appear, therefore, that there is no strong correlation between density and activation energy.

6. Conclusions

The QS technique has been successfully applied to simulate the rotation of the methyl and methoxy groups in PVME. In the case of the methyl group, the average energy barrier and the standard deviation of energy barriers compare well with data obtained from QENS.

In the case of the methoxy group it was found that a few groups totally dominate the observed dielectric response with just 4% of the groups contributing more than 90% of the relaxation strength. These groups are those with two alternative orientations of similar energy. Sampling a large number of groups allowed the highly contributing groups to be identified, and excellent agreement was found between the observed and calculated dielectric relaxation strengths.

In view of the vastly different polarizabilities of different groups, brought about by their different rotational energy profiles, the calculation of the experimental activation energy is nontrivial. A weighted average, allowing for the energy difference between alternative sites, yields an average activation energy of 18 kJ/mol, which is in good agreement with the experimentally observed values around 21 kJ/mol.

References and Notes

(1) Smith, G. D.; Borodin, O.; Paul, W. *J. Chem. Phys.* **2002**, *117*, 10350−10359.
(2) Gómez, D.; Alegría, A.; Arbe, A.; Colmenero, J. *Macromolecules* **2001**, *34*, 503−513.
(3) Rapold, R. F.; Suter, U. W.; Theororou, D. N. *Macromol. Theory Simul.* **1994**, *3*, 19−43.
(4) Tino, J.; Koren, I.; Mach, P.; Urban, J. *Macromol. Theory Simul.* **1996**, *5*, 67−74.
(5) Nicholson, T. M.; Davies, G. R. *Macromolecules* **1997**, *30*, 5501−5505.
(6) Williams, G.; Watts, D. C. *Trans Faraday Soc.* **1970**, *66*, 80−85.
(7) Chahid, A.; Alegría, A.; Colmenero, J. *Macromolecules* **1994**, *27*, 3282−3288.
(8) Berthet, J. C.; Davies, G. R. *Macromolecules*, submitted.
(9) Cendoya, I.; Alegria, A.; Alberdi, J. M.; Colmenero, J.; Grimm, H.; Richter, D.; Frick, B. *Macromolecules* **1999**, *32*, 4065−4078.
(10) Saelee, C.; Nicholson, T. M.; Davies, G. R. *Macromolecules* **2000**, *38*, 2258−2265.
(11) Sharma, S. C.; Mandelkern, L.; Stehling, F. C. *J. Polym. Sci., Part B: Polym. Lett.* **1972**, *10*, 345.
(12) Sun, H. *J. Phys. Chem. B* **1998**, *102*, 7338−7364.
(13) Andersen, H. C. *J. Chem. Phys.* **1980**, *72*, 2384−2393.
(14) Berendsen, H. J. C.; Postma, J. P. M.; van Gunsteren, W. F.; DiNola, A.; Haak, J. R. *J. Chem. Phys.* **1984**, *81*, 3684−3690.
(15) Starkweather, H. W. *Macromolecules* **1981**, *14*, 1277−1281.
(16) Arrighi, V.; Higgins, J. S.; Burgess, A. N.; Howells, W. S. *Macromolecules* **1995**, *28*, 2745−2753.
(17) Smith, G. D.; Boyd, R. H. *Macromolecules* **1992**, *25*, 1326−1332.

MA061442J